# Surface modification of cellulose nanocrystals with cetyltrimethylammonium bromide

Tiffany Abitbol, Heera Marway and, Emily D. Cranston

**KEYWORDS:** Cellulose nanocrystals, Surface modification, Surfactant ammonium surfactant, Bromide, CTAB, Ethanol

SUMMARY: Cellulose nanocrystals (CNCs) prepared by sulfuric acid hydrolysis of cotton were surface cetyltrimethylammonium modified with (CTAB). Essentially, the counterions of the CNC surface sulfate ester groups are exchanged for cetyltrimethylammonium (CTA+), which acts as a bulky, amphiphilic cation. The CTAB-modified CNCs were thoroughly purified to remove surfactant that was electrostatically bound. The surface modification could be tailored from 50 to 100% charge coupling efficiency by varying the reaction conditions. The main factor that influenced coupling efficiency was ionic strength; increasing the ionic strength screened electrostatic interactions, which led to decreased surfactant adsorption. Adsorption isotherms of CTAB on model CNC films, measured by surface plasmon resonance spectroscopy, indicated an increase in adsorbed surfactant amount with increasing bulk CTAB concentration without achieving saturation in the concentration range studied. CTABmodified CNCs were unstable in water but formed stable colloidal suspensions in ethanol, which transitioned into a continuous gel-like chiral nematic liquid crystal at relatively low concentrations (~4 wt. %) but did not phase separate into isotropic and anisotropic phases. The particle size and morphology of the CTAB-modified CNCs were unchanged compared to the native CNCs but were more thermally stable and less hydrophilic after the surface modification reaction.

#### **ADDRESSES OF THE AUTHORS:**

Tiffany Abitbol (tiffany.abitbol@mail.mcgill.ca),

Heera Marway (marwayhs@mcmaster.ca),

Emily D. Cranston (ecranst@mcmaster.ca): Department of Chemical Engineering, McMaster University, 1280 Main Street West, Hamilton, Ontario, Canada L8S 4L7 Corresponding author: Tiffany Abitbol

Cellulose nanocrystals (CNCs) are rod-shaped, highly crystalline nanoparticles extracted from natural sources of cellulose (Habibi et al. 2010, Klemm et al. 2011). The literature presents examples of CNCs produced from wood (Revol et al. 1992), cotton (Revol et al. 1994b), bamboo (Brito et al. 2012), and bacteria, using a variety of experimental routes (Revol et al. 1994a, Araki et al. 2000a, 2000b, Siqueira et al. 2010b, Leung et al. 2011, Salajková et al. 2012). The nanoparticles from different sources are similar in morphology and degree of crystallinity, and are typically 100-300 nm in length and 5-10 nm in cross-section (Habibi et al. 2010). While cellulose and CNCs are generally considered hydrophilic due to the high density of hydroxyl groups, the crystalline organization of polymer chains in nature allows for a

hydrophobic "edge" to the crystal and thus amphiphilic properties overall (Lindman et al. 2010). A number of reports have used surfactants to modify CNCs, however, the nature of the interaction between CNCs and surfactants has not been fully elucidated (Heux et al. 2000, Bonini et al. 2002, Ljungberg et al. 2005, Ljungberg et al. 2006, Bondeson, Oksman 2007a, Petersson et al. 2007, Elazzouzi-Hafraoui et al. 2009, Jackson et al. 2011, Salajková et al. 2012).

CNCs are green and biocompatible, with favourable material properties including a large specific Young's modulus (in theory, comparable to steel and Kevlar®), large aspect-ratio, a surface area of several hundred square meters per gram, light-weight, and low toxicity (Rusli et al. 2011, Lam et al. 2012). These properties make CNCs ideal for applications such as rheological modifiers (Boluk et al. 2012), emulsion stabilizers (Kalashnikova et al. 2011), templates for 3-D ordered superstructures (Shopsowitz et al. 2010, Kelly et al. 2013), drug delivery (Roman et al. 2009), and scaffolds for tissue engineering (Dugan et al. 2010). However, CNCs are most often cited for their potential as reinforcement agents in polymer systems, where particlematrix interactions must be optimized and CNCs evenly dispersed to take full advantage of their surface-area-tovolume ratio (Dufresne 2010). The use of CNCs in hydrophobic systems thus requires surface modification. Different approaches have been used to hydrophobize CNCs, including small molecule covalent modification (Grunert, Winter 2002, Yuan et al. 2006, Junior de Menezes et al. 2009), silylation (Goussé et al. 2002, Goussé et al. 2004), surfactant adsorption (Heux et al. 2000, Kim et al. 2009, Salajková et al. 2012) and polymer grafting reactions (Hubbe et al. 2008, Siqueira et al. 2010a, Moon et al. 2011, Peng et al. 2011).

While many of the proposed applications for CNCs are solid nanocomposites, others are liquid-based. These require homogeneous dispersion of CNCs in solvents, often in the presence of other polymers, particles and dispersants. Unmodified cellulose nanocrystals form stable colloidal suspensions in water as predicted by DLVO theory (Verwey, Overbeek 1948, Derjaguin, Landau 1993). The double-layer electrostatic repulsion contribution to DLVO comes from surface charge groups on CNCs; the exact surface chemistry is controlled by the CNC production method. Most commonly, CNCs are prepared by sulfuric acid hydrolysis and possess anionic sulfate half-ester groups on their surface (Dong et al. 1998). The  $pK_a$  of the grafted sulfate half-ester is estimated at 2.5, allowing for stable suspensions over a wide pH range (Cranston et al. 2010, Wang et al. 2011). CNCs prepared by oxidation with ammonium persulfate (Leung et al. 2011), or 2,2,6,6-tetramethylpiperidine 1oxyl (TEMPO) (Salajková et al. 2012) have anionic carboxylic acid groups on the surface. Conversely, HCl hydrolysis of cellulose yields uncharged (and unstable) CNCs, however, grafting polymers to induce steric stabilization has been a successful post-production modification (Araki et al. 2000a, Kloser, Gray 2010). Ideally, CNCs would be stable in a variety of polar and non-polar media facilitating chemical reactions, dispersibility in water and solvent-borne systems, and extending material processing possibilities.

Surfactant adsorption to CNCs offers a facile and promising route to alter the surface chemistry and tailor colloidal stability in an industrially feasible process. Heux and co-workers were the first to achieve stable dispersions of surfactant-modified CNCs in toluene and cyclohexane using the surfactant Beycostat NA (BNA), a phosphoric ester of polyoxyethylene (9) nonylphenyl ether (Heux et al. 2000, Bonini et al. 2002, Elazzouzi-Hafraoui et al. 2009, Brito et al. 2012). They also observed the first instance of chiral nematic liquid crystalline ordering and phase separation of CNCs in an organic solvent; this behaviour is characteristic of aqueous suspensions of native CNCs and supports potential optical applications such as polarization filters, pigments and anti-counterfeit coatings (Revol et al. 1997). Building on that work, polymer composites with CNCs and BNA were processed in chloroform and exhibited remarkably good dispersion of CNCs within the matrix (Bondeson, Oksman 2007b, Bondeson, Oksman 2007a, Petersson et al. 2007). More recently, Salajková et al. (2012) achieved carboxylated CNC suspensions in cationic toluene through modification with stearyltrimethylammonium chloride (STAC), inspiring the current work.

We have chosen to surface-modify CNCs with cetyltrimethylammonium bromide (CTAB), a common cationic surfactant with a quaternary ammonium head and a C16 alkyl tail. CTAB and CNCs have been investigated together previously: CTAB was able to couple hydrophobic anti-cancer drugs to CNCs and deliver controlled drug release (Jackson et al. 2011), and CTAB was found to aid in CNC-templated metal nanoparticle synthesis (Padalkar et al. 2010). The previous reports of surfactant modified CNCs involve the mixing of surfactants and CNCs in water but without studying the effect of adsorption reaction conditions in detail, and without discussion of the adsorption mechanism or the role of unbound surfactant in solution. Similarly, cellulose-surfactant interactions for non-CNC celluloses have been studied and highlight the importance of factors such as cellulose surface charge density, surfactant hydrophobic tail length, ionic strength and surfactant concentration (Alila et al. 2005, Syverud et al. 2011, Xhanari et al. 2011), but to the best of our knowledge, such parameters have not been investigated in CNC-surfactant systems.

In this work, we explore the surface modification reaction of sulfated CNCs (both commercially available and lab-made) with CTAB, taking into account the effects of reaction conditions including CTAB:CNC ratio, CTAB concentration, pH, and ionic strength. The degree of surface modification and resulting hydrophobic nature of the CNCs is evaluated in terms of chemical composition, particle morphology, dispersion in non-

aqueous solvents, liquid crystalline phase behavior, contact angle and rheological properties. We believe this to be the first report of the surface modification of sulfated CNCs with quaternary ammonium surfactants. The adsorption of CTAB onto CNCs in aqueous suspension is compared to adsorption onto solid CNC films using surface plasmon resonance spectroscopy (SPR). This fundamental study of CNC–surfactant interactions is timely given the speculation that current industrial R&D is focused on developing commercial CNC products which will likely take advantage of surfactant modification routes to enhance the colloidal stability and dispersibility of CNCs.

# **Materials and Methods**

#### **Materials**

Commercially-produced CNCs, from sulfuric acid hydrolysis of Whatman cotton filter paper, were obtained from Alberta Innovates Technology Futures as a freezedried powder. Samples were briefly sonicated (Branson SLPt, 60% output) prior to usage. Tetrahydrofuran (reagent grade, Caledon), toluene (99.9% purity, Fischer Scientific Inc.), and anhydrous ethanol (Commercial Alcohols, Brampton, ON) were used without further drying or purification. CTAB from Sigma-Aldrich and poly(allyamine hydrochloride) (MW = 120-200 kDa) from Polysciences were used as received. The lab-made CNCs were prepared from Whatman cotton ashless clippings filter aid (GE Healthcare, UK).

## **CNC** preparation

To prepare "lab-made" CNCs, the ashless clippings were torn into small squares and blended into a fluffy, white powder in a standard household blender (Magic Bullet brand). The powder was dried at 50°C for 1 h prior to the reaction. The sulfuric acid hydrolysis followed the same general procedure that has been published elsewhere (Beck-Candanedo et al. 2005) with an acid to cotton ratio of 17.5 ml/g, an acid concentration of 64 wt. %, and a 45 min reaction at 45°C, with acid removal achieved by extensive dialysis (Spectra/Por dialysis tubes, 12-14 kDa molecular weight cut-off) against Milli-Q water until the pH of the external reservoir was stable over the last few water changes (~3 weeks/40 g batch). A comparison of lab-made CNCs and the commercial CNCs used in this work is presented in *Table 1*.

#### Conductometric titration

Conductometric titrations to quantify the acid content of the lab-made CNCs were performed using a thoroughly dialyzed sample, without the use of ion-exchange resin (Abitbol et al. 2013). The commercial CNCs were also titrated in this manner, however cationic acid exchange resin (Dowex® Marathon<sup>TM</sup> C hydrogen form, Sigma-Aldrich) was employed to convert the sodium-form suspension to acid-form. The suspensions were titrated against dilute NaOH (2 mM), and the acid content was related to the surface sulfur content of the CNCs as described by Dong et al. (1998).

#### **CTAB** modification of CNCs

The reaction conditions for the CNC surface modifycations are presented in Table 2 and were based on the work of Salajkovà et al. (2012), who modified TEMPOoxidized CNCs with STAC. As indicated, the mole ratio of CTAB to CNC sulfate ester groups, surfactant concentration, scale and pH of the reaction were varied. The critical micelle concentration (cmc) of CTAB is ~1 mM (McDermott et al. 1993). CTAB-modification of the commercial CNCs was performed at a relatively large scale, using 5 g of CNCs (1 wt. % suspension, pH adjusted to 10 through the addition of 1 M NaOH), and a 1 wt. % aqueous CTAB solution (2:1 CTAB to sulfur mol ratio). The suspension was slowly added into the CTAB solution, and the foamy mixture was maintained at 60°C for 3 hours, after which the heat was turned off and the reaction was left stirring at room temperature overnight. The other two reactions used lab-made CNCs and a 4:1 CTAB to sulfur mol ratio (with or without pH adjustment), and were similarly executed but at a smaller scale, using 0.5 g of CNCs (0.1 wt. % suspension), and a 0.1 wt. % CTAB solution. Unbound CTAB was removed by a combination of ultracentrifugation (20, 000 g, 10 min, 1-3 cycles) and dialysis (10-15 water changes). The samples were then either freeze-dried or solvent exchanged using a Millipore solvent-resistant stirred-cell by repeatedly concentrating the sample from 300 ml to 50 m, and topping back up to maximum volume with ethanol. The terminology used for surfactant modified CNCs is CTA-CNCs because the CNC sulfate ester group counterions are exchanged from H<sup>+</sup> or Na<sup>+</sup> (depending on the starting pH) to cetyltrimethylammonium (CTA<sup>+</sup>).

## Elemental analysis

Elemental analysis was performed by Micro Analysis Inc. (Wilmington, DE). The materials were combusted in a

pure oxygen environment and thermal conductivity was used to separate and detect elements. Samples of commercial CNCs before and after dialysis were analyzed for sulfur, and the CTAB modified samples were analyzed for sulfur and nitrogen. The results from elemental analysis are an average of two independent measurements and are given to one significant digit.

## Fourier-transform infrared (FTIR) spectroscopy

KBr pellets were prepared using a Carver Inc. hydraulic press (model 3853-0) at 10,000 psi and the spectra were obtained using a Nicolet 6700 FTIR spectrometer (Thermo Scientific). The resultant spectra were baseline corrected and represent an average of 32 scans, with a resolution of 4 cm<sup>-1</sup>.

## Thermogravimetric analysis (TGA)

The thermal decomposition of CNCs before and after surfactant modification was explored by heating the samples in air (ca. 20 mg of freeze dried powder), using a Netzsch STA-409 thermoanalyzer. The samples were heated at a rate of 5K/min, from 35-800°C.

## Dynamic light scattering (DLS)

DLS measurements were obtained using a Malvern Zetasizer Nano-S. Results are reported as a z-average diameter, which does not accurately represent the physical size of the rod-shaped nanoparticles, but is useful for comparison between different samples. The native and modified CNC samples were diluted in the appropriate solvent to a concentration of 0.025 wt. %, and 3 independent measurements were obtained for each sample, at 25°C, with 5 runs per measurement. For the modified samples measured in ethanol, it was necessary to change the dispersant from water to ethanol, with refractive index = 1.361 and viscosity = 1.074 mPa·s (CRC Handbook of Chemistry and Physics 2013-2014).

Table 1 - Physical properties of native CNCs: commercial CNCs and lab-made CNCs prepared from cotton.

	Commercial CNCs	Lab-made CNCs	
Cellulose source	cotton filter paper	cotton ashless clippings filter aid	
AFM size (nm)	$115 \pm 8 \times 8.0 \pm 0.5$	$120 \pm 10 \times 6.6 \pm 0.8$	
DLS "size" (nm)	$80 \pm 3$	81 ± 2	
Mobility (×10-8 m <sup>2</sup> /Vs)	-2.85 (0.13)	-3.24 (0.05)	
%Sulfur (wt. %)*	$0.72 \pm 0.01$	$0.648 \pm 0.003$	
Surface charge density (e/nm²)§	0.43	0.32	

<sup>\*</sup> Initial %S values prior to CTAB modification were measured by conductometric titration.

Table 2 - Summary of reaction conditions for modifying CNCs with CTAB. All reactions were for 3 hours at 60 °C, followed by stirring overnight at room temperature. Note that CNC concentration and suspension pH refer to the concentration and pH of the initial suspension before it was combined with CTAB, whereas the CTAB molarity refers to the final concentration of CTAB after the CNCs were added.

Reaction	CNC type	CNC concentration (wt. %)	Suspension pH	mol CTAB:mol sulfur	CTAB molarity (mM)
1	Commercial	1	10	2:1	4.4
2	Lab-made	0.5	10	4:1	0.8
3	Lab-made	0.5	4	4:1	0.8

<sup>§</sup> Calculated based on the AFM dimensions.

#### **Electrophoretic mobility**

The electrophoretic mobility of native CNC samples was measured using a Zeta Potential ZetaPlus analyzer. The samples were diluted to 0.25 wt. % in Milli-Q water and spiked with concentrated NaCl (1 M) to achieve an overall NaCl concentration of 10 mM. Each sample was measured 10 times, with 15 cycles per measurement. The results are reported as the average of the 10 measurements, with the associated standard deviation provided in brackets.

#### Dispersibility

The dispersibility of native CNCs was evaluated in Milli-Q water, ethanol, THF, and toluene as follows: freezedried powder (0.01 g) was added to solvent (10 ml), and sonicated at 60% output for 30 min total (Branson 450 sonifier) in 5 min intervals to avoid overheating of the samples. The CTAB-modified samples were prepared using the same procedure described above, except for the ethanol dispersion which was accomplished by solvent exchange in a Millipore solvent-resistant stirred-cell operated at 20 psi, followed by a 1-2 min sonication treatment per 100 ml sample. The dispersibility of modified CNCs in different solvents was assessed visually, and where possible (i.e., for stable suspensions) by DLS.

#### Contact angle

Static advancing water contact angle measurements were obtained using a Krüss Drop Shape Analysis system. Contact angle measurements were obtained for films of CNCs deposited onto silicon wafers (cleaned either by acid piranha, or rinsed in Milli-Q water, 95% ethanol, followed by a 20 min UV-O<sub>3</sub> treatment). Films of native CNCs (Na-form) were prepared by first spin-coating PAH (0.1 wt. %) onto the cleaned wafer, rinsing off excess by spin-coating a droplet of water, followed by the deposition of the CNC suspension (2 wt. %). The CTAB modified CNCs were spin-coated from ethanolic suspension directly onto a cleaned Si wafer from a 2 wt. % suspension with no PAH adlayer. The spin-coating steps were for 30 s at 4000 rpm. The films were placed in the oven overnight at 80 °C prior to measurement. The results are reported as an average of 3-6 measurements.

#### Atomic force microscopy (AFM)

A Nanoscope IIIA AFM with E scanner (Bruker AXS) was used to image CNCs before and after surface modification. Dilute samples (0.001-0.01 wt. %) were deposited onto cleaned silicon wafers (20 min UV/O<sub>3</sub> treatment) by spin-coating (4000 rpm, 30 s). CTAB modified samples in ethanol were deposited directly onto the silicon wafer, whereas a PAH (0.1 wt. %) precursor layer was used for the native CNC samples.

# Polarized optical microscopy

Samples of CTA-CNCs in ethanol for polarized optical microscopy were prepared by slow evaporation in rectangular, borosilicate microslides manufactured by Vitrocom (1  $\times$  10 mm inner diameter, 100 mm length). One end of the tube was sealed, and the other end was left open. To prevent evaporation, once the desired concentration was achieved, the open end was covered

with Parafilm®. Polarized optical microscope images were obtained using a Nikon Eclipse LV100N POL microscope and an Infinity 1 color camera. A 530 nm waveplate was inserted into the light path between the sample and analyzer.

## Rheology

The viscosity as a function of shear stress was measured for CNCs in water and CTA-CNCs in ethanol, ranging in concentration from 1-4 wt. % using an ATS Rheo-Systems Stresstech HR rheometer in cone and plate geometry. Three independent measurements were obtained for each sample. To prevent evaporation of solvent over the course of the measurement (ca. 60 s), the gap between the cone and plate was overfilled so that the overflow solvent edge would evaporate first and the volume between the cone and plate would be unaffected.

## Surface plasmon resonance (SPR) spectrometry

The interaction of CTAB with CNC model surfaces was explored in situ using a SPR Navi<sup>TM</sup> 200 (BioNavis, Finland). An increase in adsorbed layer thickness on an SPR sensor is manifested as a shift in the optical resonance properties of the sensor. This shift is detected as an increase in the "SPR angle" where the reflected light intensity is at its minimum. Reflected intensity of light at 670 nm as a function of incident angle was collected over the angular range of 40° to 80° such that the SPR angle position and the angle of total internal reflection (TIR) were both detected (Liang et al. 2010). The TIR angle is related to the refractive index of the surrounding medium and if the medium changes, the TIR shifts and the SPR angle also shifts by the same amount. As such, it is important to subtract the TIR from the SPR peak angle to ensure that measured angular shifts are due to adsorbed material alone. SPR data is presented as a change in SPR angle minus TIR,  $\Delta$ (SPR angle – TIR angle), as a function of adsorption time.

Titania-coated gold SPR sensors (SPR102-TIO2, BioNavis) were rinsed in ethanol and UV/O<sub>3</sub> treated for 20 min. CNC model films were deposited on the sensors by spin-coating a 1 wt. % suspension of lab-made CNCs at 4000 rpm for 30 s. CTAB at 23.4 °C was flowed over the CNC films at 100  $\mu$ l/min and SPR data was collected until an adsorption plateau ( $\Gamma$ ) was reached (defined as a change in SPR peak angle of less than 0.1° over 5 min). After CTAB adsorption, the samples were rinsed *in situ* with Milli-Q water until no further change in SPR peak angle was observed. This process was carried out for CTAB concentrations of 0.01, 0.5, 2, and 4 mM.

#### Results and Discussion

## Effect of reaction conditions

The effect of reaction conditions on the surface modification of CNCs with CTAB was examined. Primarily, the mole ratio of surfactant to surface sulfate ester groups, pH, and ionic strength were controlled. Secondary effects depending on whether the surfactant concentration during the reaction was above or below the cmc were also monitored. Two types of sulfated CNCs, lab-made and commercial source, were characterized (*Table 1*) and reacted according to the conditions

presented in *Table 2*. *Fig 1* shows the two types of reactions: (A) pH-adjusted CNC suspensions reacted with CTAB at or above the cmc, which corresponds to reactions 1 and 2 in *Table 2*, and (B) reactions carried out with CTAB concentration close to the cmc with no pH adjustment of CNC suspensions, which corresponds to reaction 3 in *Table 2*.

After the reaction of CTAB with CNCs, CTA-CNCs were no longer colloidally stable in water and settled to the bottom of the vessel as a fluffy white powder. Extensive purification was then undertaken to remove unbound surfactant. A combination of ultracentrifugation and dialysis was employed to ensure further characterization results and observed phenomena were due to surface modified CNCs, and not an interplay between colloidal particles and free surfactant. There was no observable difference in the modified CNC suspensions after purification.

#### Effect of CTAB:sulfur mole ratio

Assuming that the interaction between CTAB and CNCs is electrostatic in nature, we define the "coupling efficiency" as the percent of surface sulfate ester groups that have had their counterion exchanged for CTA<sup>+</sup>. Elemental analysis was used to determine the nitrogen and sulfur contents of the purified reactions, representing the amounts of surfactant and sulfate ester groups, respectively. Results are presented in *Table 3* and

indicate that changing the mole ratio of CTAB:sulfur from 2:1 to 4:1 at pH 10 leads to an increase in coupling efficiency, from approximately one-half to two-thirds. The complete exchange of CNC counterions for CTA<sup>+</sup> was achieved with a 4:1 mol ratio at pH 4. However, we consider the effect of mole ratio to be minor, since in this case the surfactant concentration and ionic strength were not held constant.

#### Effect of CTAB concentration

Typically, the equilibrium adsorption of cationic surfactants from aqueous solution onto negatively charged cellulosic surfaces increases with increasing bulk surfactant concentration (Alila et al. 2005, Penfold et al. 2007, Syverud et al. 2011, Xhanari et al. 2011, Dhar et al. 2012). The difference in coupling efficiency between CTA-CNCs-50% and CTA-CNCs-70% seems to follow the opposite trend since the CTAB concentration was 5.5 times greater for CTA-CNCs-50% (Table 2). The key to understanding this apparent discrepancy is to consider that in studies where the adsorption is measured in solution, the equilibrium between the bulk and surface concentrations of surfactant dictates the adsorption, whereas in the current scenario, the equilibrium is shifted toward desorption by the washing steps during the postmodification purification.

Table 3 - Characterization of CTAB-modified CNCs including nitrogen and sulfur content from elemental analysis, and the calculated coupling efficiency. Reaction numbers refer to reaction conditions presented in *Table 2*.

	Reaction 1 2:1, pH 10	Reaction 2 4:1, pH 10	Reaction 3 4:1, pH 4
Sample name	CTA-CNCs-50%	CTA-CNCs-70%	CTA-CNCs-100%
%S after modification (wt. %)	0.64	0.60	0.62
%N after modification (wt. %)	0.15	0.19	0.28
Coupling efficiency: mol N/ mol S x 100 %*	50	70	100

<sup>\*</sup> Coupling efficiencies are reported to one significant digit.

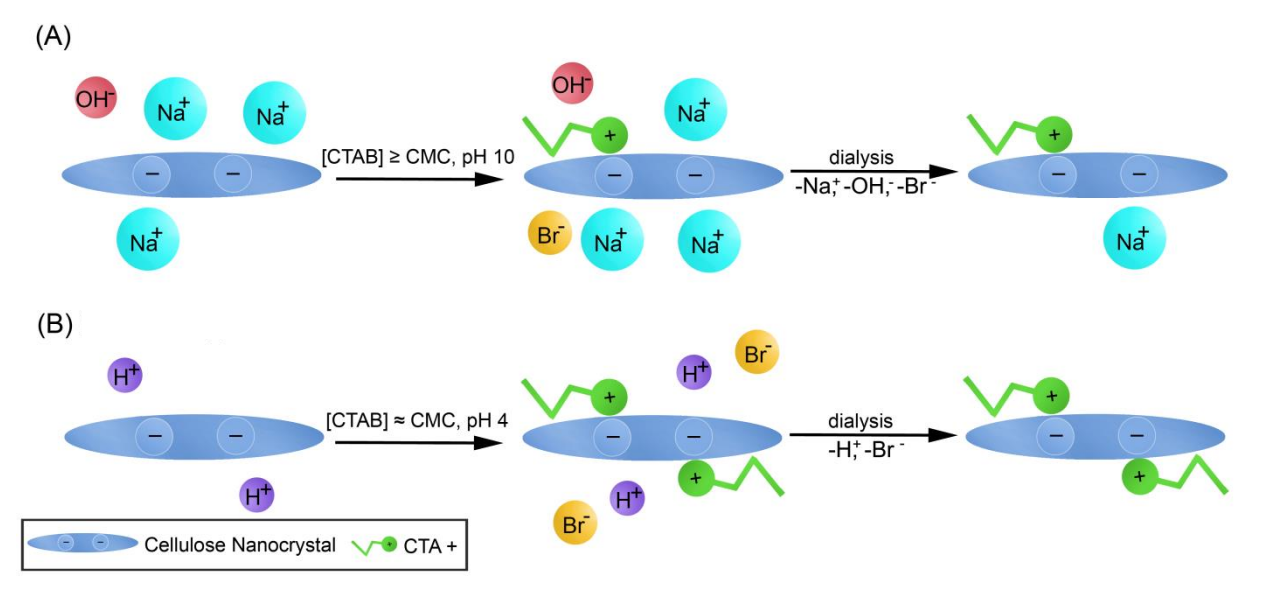


Fig 1 - Schematic representation of the two types of CTAB-modification reactions used in this work: (A) [CTAB] ≥ cmc and pH 10 CNC suspension (reactions 1 and 2), and (B) [CTAB] ≈ cmc and pH 4 CNC suspension (reaction 3).

#### Effect of pH and ionic strength

In previous work by Salajkova et al. (2012), alkaline reaction conditions were employed to ensure complete deprotonation of the anionic surface-grafted COOH groups on CNCs which have an apparent  $pK_a$  of approximately 5 (Notley, Norgren 2006). In our case, the charged groups are sulfate half esters which are deprotonated above pH 2.5 (Cranston et al. 2010, Wang et al. 2011). As such, the effect of carrying out the reaction at pH 4 or pH 10 is minimal from a surface charge density argument. It is likely that the increased ionic strength due to added NaOH at pH 10 is responsible for the lower coupling efficiency in reaction 2 vs. reaction 3 since all other reaction parameters were constant. The ionic strength due to added base at pH 10 is essentially double the ionic strength at pH 4 when one considers that the charged CNCs themselves contribute to the ionic strength. To achieve a pH 10 suspension, the NaOH first neutralized the acidic CNCs, and then excess NaOH was added to give a pH 10 suspension.

Alila et al. (2005) studied the effect of ionic strength on the adsorption of cationic surfactants onto cellulose fibers as a function of surfactant concentration; an increase in ionic strength at low surfactant concentrations hindered electrostatic adsorption due to charge screening. However, at high surfactant concentrations, an increase in ionic strength led to denser packing due to shielding of the repulsive interactions between cationic head groups. Assuming we are in a "low surfactant concentration range" for this system, the same trend is observed here. We also note that compared to the TEMPO-oxidized surfaces of the aforementioned work, the surface charge density on our CNCs is relatively low such that surfactant molecules ionically-bound to sulfate ester groups should experience minimal "inter-surfactant" electrostatic repulsion. Similarly, the adsorption of tetradecyltrimethylammonium bromide (TTAB) on sulfated CNCs also showed that added salt screened electrostatic interactions between surfactant heads and CNC charge groups (Dhar et al. 2012).

When reactions carried out at the same pH are compared (reactions 1 and 2), we see that a higher ionic strength hinders electrostatic adsorption because of charge screening. Reaction 1 has a higher ionic strength due to an overall higher concentration of both CNCs and surfactant and has the lowest coupling efficiency as a result. In our view, ionic strength is the main factor that determines the amount of electrostatically bound surfactant, whereas the influence of CTAB:sulfur mol ratio and CTAB concentration is relatively minor at the conditions employed in this work (i.e., concentration ≥ cmc, and 2:1 or 4:1 CTAB:sulfur mol ratios).

#### Effect of rinsing

In terms of the post-reaction washing of excess surfactant, it seems that if there are surfactant molecules adsorbed via hydrophobic interactions, they are rinsed away. Conversely, the ionic bond between CTA<sup>+</sup> and the anionic sulfate ester group is more permanent and not affected by the rinsing step. This is supported by AFM studies of the adsorption of cetyltrimethyl-ammonium chloride (CTACl) onto silica surfaces which showed that

the micelle structures obtained by adsorption from 2 mM CTACl immediately washed away after rinsing with water, whereas electrostatically bound surfactant did not desorb as quickly (Liu et al. 2001). In addition, it was suggested that the ionic bond between CTA<sup>+</sup> and anionic silica sites was strengthened as the counterions originally associated with the surface and surfactant were washed away.

The molecular picture of our CTA-CNCs prepared through adsorption and rinsing is that 50-100% of the CNC surface charge groups are coupled with one surfactant molecule where the hydrophobic tails of the surfactant lie flat against the CNC surface to minimize contact with water. The spacing between charged groups on the CNCs likely plays a significant role: we have 1 sulfate half-ester per 12-14 surface anhydroglucose units corresponding to 2.3-3.1 nm² per charged groups (Kan et al. 2013). A fully extended CTAB tail is about 2 nm long therefore the hydrophobic tails cannot easily associate or drive non-electrostatic adsorption of surfactant.

The FTIR spectra (Fig 2) and TGA (Fig 3) further support the surface modification reactions although only slight changes are observed in the modified CNC samples compared to native CNCs. The FTIR spectra of CTA-CNCs had a small peak at ~1480 cm<sup>-1</sup> attributed to the trimethyl groups of the quaternary ammonium (Salajková et al. 2012). This peak is arguably more apparent for CTA-CNCs-100% than CTA-CNCs-50%, as would be expected. The surface modification of CNCs led to a more thermally stable nanoparticle; the onset of thermal degradation shifted from 277 to 307°C after CTAB adsorption (Fig 3 inset).

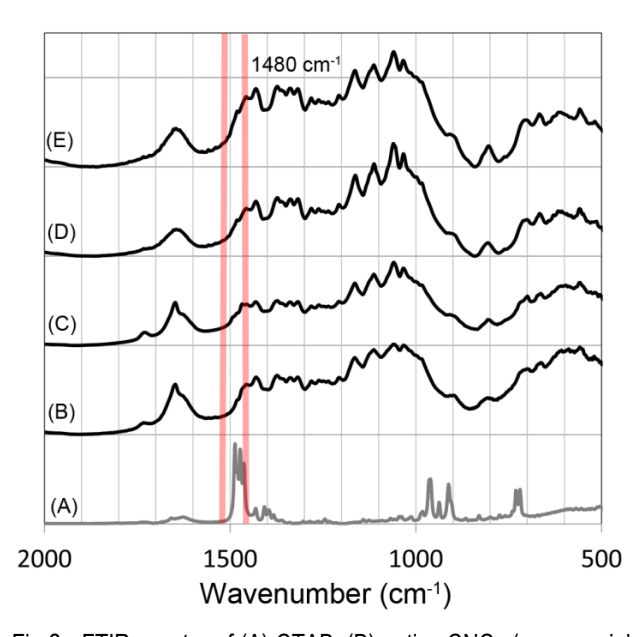


Fig 2 - FTIR spectra of (A) CTAB, (B) native CNCs (commercial source) and CTAB-modified samples: (C) CTA-CNCs-50%, (D) CTA-CNCs-70%, and (E) CTA-CNCs-100%.

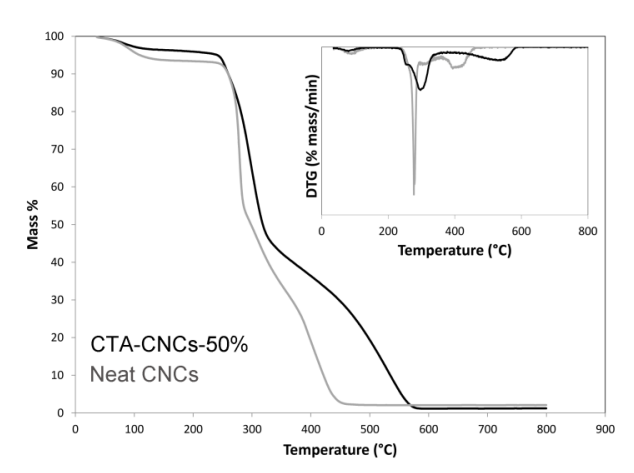


Fig 3 - TGA (main figure) and DTG (inset) of native (commercial source) and CTA-CNCs-50%.

## **CNC-surfactant adsorption isotherm**

The adsorption of CTAB onto model cellulose surfaces, prepared by spin-coating neat CNCs onto titania SPR sensors, was studied by SPR. The resultant isotherms are shown in  $Fig\ 4$  whereby a change in  $\Delta(\text{SPR angle} - \text{TIR angle})$  is proportional to the adsorbed CTAB layer thickness.

As mentioned above, this general trend of increased maximum adsorbed amount ( $\Gamma$ ) with bulk surfactant concentration on cellulose has been seen by others (Alila et al. 2005, Alila et al. 2007, Penfold et al. 2007, Syverud et al. 2011, Xhanari et al. 2011, Dhar et al. 2012). After 10 min of adsorption (Fig~4A), the sensorgrams for the higher CTAB concentrations have essentially reached a plateau, whereas longer times (>30 min) are required to achieve steady-state for the 0.01 and 0.5 mM CTAB solutions.

The amount of adsorbed CTAB increases more or less steadily over the CTAB concentration range from 0.01 to 4 mM (Fig 4B). This implies that the surface has not achieved full saturation at 4 mM. In this system, full saturation would likely surpass 100% compensation and include hydrophobic surfactant interactions. For example, Dhar et al. (2012) observed cooperative binding of TTAB to CNCs from the comparison of isothermal titration calorimetry (ITC) and zeta-potential results; three distinct regimes in the adsorption isotherm were identified: (1) electrostatic adsorption at low concentrations (i.e., non-cooperative binding), (2) cooperative surfactant binding and CNC aggregation at intermediate concentrations, and (3) micellization of free surfactants at concentrations approaching the cmc.

To relate the SPR adsorption experiment to the modification reaction with CNCs, it was necessary to rinse the SPR sensors after the adsorption had plateaued to look at the amount of surfactant remaining. The percent of surfactant washed off with rinsing ranged from 40-50% for CNC films that adsorbed CTAB from 0.01 and 0.5 mM concentrations, whereas 70-80% of the CTAB was desorbed from the CNC films adsorbed from 2 and 4 mM surfactant solutions. Based on the above discussion, the CTAB that desorbed is likely from cooperative surfactant binding. The greater desorption

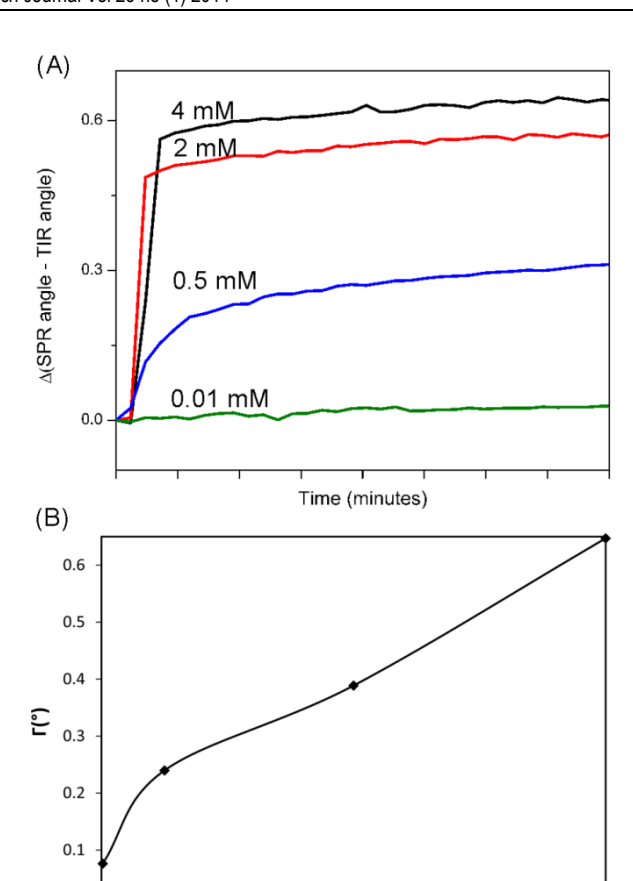


Fig 4 - (A) SPR sensorgrams showing the first 10 min of adsorption for the different CTAB concentrations studied: 0.01, 0.5, 2, and 4 mM. Compared to the steady increase in adsorbed amount, from 0.08 to 0.65°, with increasing bulk CTAB concentration, the amount of CTAB remaining on the surface after rinsing was 0.05–0.22° with no concentration dependent trend. (B) The CTAB–CNC adsorption isotherm (line is a guide for the eye).

CTAB concentration (mM)

observed at the higher CTAB concentrations is related to the increase in hydrophobic surfactant interactions with increasing CTAB concentration (i.e., more non-electrostatically bound surfactant is present and able to be washed off). The similar amount of CTAB remaining on the films after rinsing can be attributed to electrostatically bound surfactant, which should be the same for substrates having the same surface coverage of nanocrystals with the same surface charge density.

# **Dispersibility of CTA-CNCs**

0

The dispersibility of CTAB-modified CNCs in solvents of decreasing polarity is presented in *Table 4* and *Fig 5*. Stable suspensions of CTA-CNCs were obtained in ethanol, but not in water, THF or toluene. Suspensions in water were turbid, in THF a translucent gel-like layer formed at the bottom of the mixture, and in toluene the CTA-CNCs remained in powder form. We note that the ethanol suspensions were prepared differently from the other mixtures; solvent exchange vs. re-dispersion with

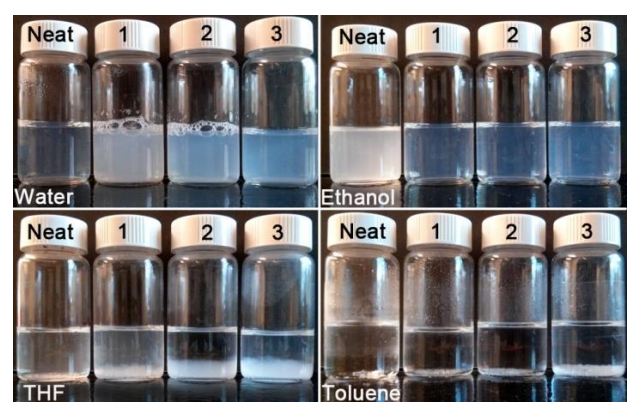


Fig 5 - Photographs of 0.1 wt. % neat CNCs (commerical source) and CTAB-modified CNCs dispersed in water, ethanol, THF and toluene by a sonication treatment: (1) CTA-CNCs-50%, (2) CTA-CNCs-70%, and (3) CTA-CNCs-100%. The photograph was taken after the suspensions were left standing for over 24 hours.

sonication for freeze dried powders. That being said, we apparent difference between ethanolic no suspensions from either method, and it was more efficient to disperse and concentrate large volumes of CNCs by solvent exchange using ultrafiltration. The CTA-CNCs exhibited reduced stability in water because the charged surface sites that impart electrostatic stabilization in water were blocked by CTAB, and the surfaces of the CNCs were made partially hydrophobic. The limited dispersibility in THF and toluene is due to insufficient CTAB as a result of the low surface charge density of the substrate. Furthermore, the C16 surfactant tail may not be hydrophobic enough to stabilize CNCs in such solvents. A longer alkyl chain, such as the C18 of STAC has been shown to be long enough to impart stability in toluene when cellulose surface charge density was still relatively low, albeit higher than the surface charge density used in this work (Salajková et al. 2012).

For solvents that supported stable suspensions of CTA-CNCs, "apparent" particle size was measured by DLS for comparison purposes (*Table 4*). The increase in DLS size for CTA-CNCs in ethanol, compared to native CNCs in water, is attributed to the extension of the surfactant tails from the surface of the CNCs. However, for dried CNCs and CTA-CNCs imaged by AFM (*Fig 6*), no significant change in morphology or particle dimensions are observed (i.e., modified CNCs were 8.8-10.2 nm in height and 111-124 nm in length).

Suspension stability of CTA-CNCs in ethanol could also be inferred from AFM images (Fig 6); the relatively good dispersion achieved by the deposition of modified samples directly onto silicon wafers, without requiring a cationic polymer precursor layer, is indicative of the increased hydrophobicity of the particles. The AFM results do however seem to indicate less than perfect dispersion since small, lateral agglomerates are apparent, particularly in images of CTA-CNCs-70% and CTA-CNCs-100%. Possibly the agglomerates seen in the more modified samples are from the association of CTAB tails as the particles are brought closer together during solvent evaporation.

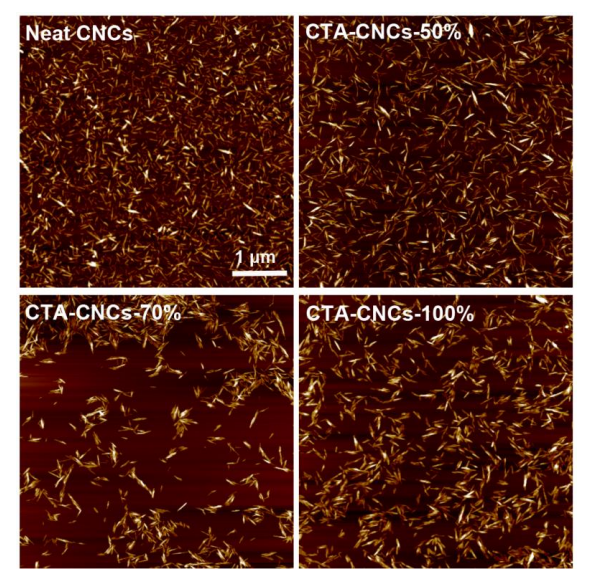


Fig 6 - AFM height images of neat CNCs (commercial source) spin-coated from aqueous suspension, and CTAB- modified CNCs spin-coated from ethanolic suspension. (Height scale  $\sim 20$  nm and scan size  $5 \times 5$  µm.)

## Contact angle

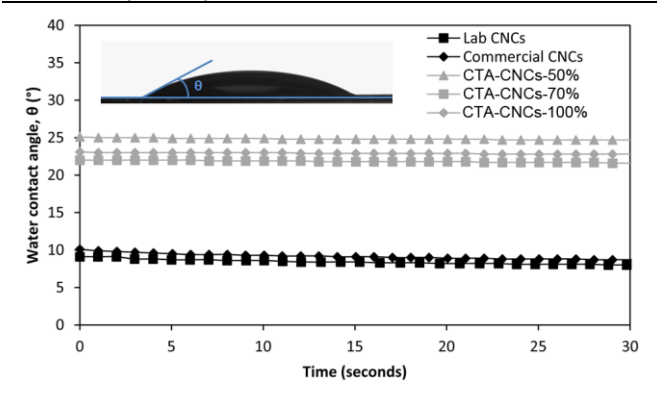
In general, the contact angle of CNC surfaces modified with cationic surfactants is a function of the amount of electrostatically bound surfactant (determined by surface charge density), the length of the alkyl tail, and the conformation of the surfactant at the solid-air interface. The contact angle for water was higher on films prepared from CTAB-modified CNCs compared to neat CNC films but did not indicate a fully hydrophobic surface (Fig 7). The top panel in Fig 7 shows the evolution of the water contact angle as a function of time; both neat CNCs and CTAB-modified CNCs showed a decrease in contact angle with time, however, the decreasing slope was steeper for the neat CNCs due to enhanced water penetration into the more hydrophilic surface.

The water contact angle of our neat CNC films  $(8.6^{\circ} \pm 0.4^{\circ} \text{ for lab CNCs}, 8.5^{\circ} \pm 0.4^{\circ} \text{ for commercial})$ CNCs) is similar to the  $13.1^{\circ} \pm 0.6^{\circ}$  obtained by Dankovich and Gray (2011) for spin-coated CNCs films, as is the steady decrease in water contact angle with time. Salajková et al. (2012) achieved a water contact angle on model films made from STAC-modified carboxylated CNCs of 48°, compared to 12° for neat CNCs. Salajková et al. (2012) also noted that washing the STAC-CNC coated surface in toluene prior to contact angle measurement further increased the contact angle to 71°. This behavior was attributed to the rinsing away of excess surfactant and to the reorganization of admicelles, so that the hydrophobic tails extend from the surface. In contrast, the highest contact angle measured for CTA-CNCs was  $27^{\circ} \pm 1^{\circ}$ .

Comparing the STAC-CNC system to the work presented here, it seems that an increase in alkyl chain length from 16 to 18 carbons, and an increase in surface charge from ~0.2 mmol/g (our sulfated CNCs) to 1.5 mmol/g (TEMPO-oxidized CNCs used by Salajková et al.), can increase the water contact angle by more than  $20^{\circ}$ .

Table 4 - Dispersibility of CTAB-modified CNCs in different solvents assessed visually (see accompanying photographs in *Fig* 5). DLS was measured for stable suspensions and apparent particle sizes are indicated in brackets. The dielectric constants (ε) are provided for reference adjacent to the solvent name (CRC Handbook of Chemistry and Physics 2013-2014).

Stable in	Native CNCs	CTA-CNCs-50%	CTA-CNCs-70%	CTA-CNCs-100%
Water ( $\varepsilon_r$ = 80.1)	Yes (80 ± 3 nm)	Partial	Partial	Partial
Ethanol ( $\varepsilon_r = 25.3$ )	Partial	Yes (96 ± 1 nm)	Yes $(93 \pm 6 \text{ nm})$	Yes $(97 \pm 2 \text{ nm})$
THF ( $\varepsilon_{\rm r}$ = 7.5)	No	Partial	Partial	Partial
Toluene ( $\varepsilon_{\rm r} = 2.4$ )	No	No	No	No



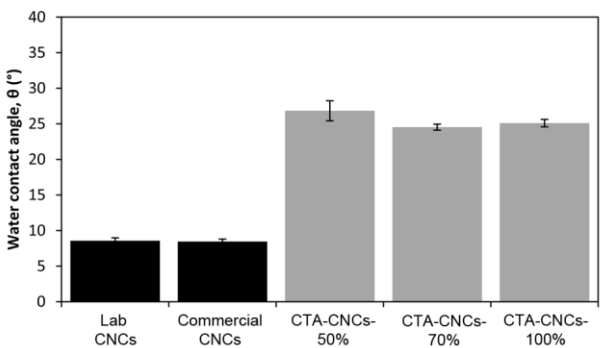


Fig 7 - Representative curves for water contact angle as a function of time (top panel), and average values at t=0 s with associated error interval (bottom panel) for neat CNCs and CTAB-modified CNCs.

## Liquid crystalline behaviour

The phase behavior of CTA-CNCs-50% in ethanol was studied as the suspension was concentrated by ambient evaporation. The suspensions became more viscous, and showed texture between crossed polarizers beginning at ~2 wt. %, and the formation of a gel-like chiral nematic phase at ~4 wt. %. This is in contrast to the neat commercial CNCs (used to make CTA-CNCs-50%), which began to phase separate only at ~6-7 wt. %.

Fig 8a shows a microslide containing an ethanolic suspension of CTA-CNCs-50% that had been slowly concentrated from 3.5 to 6 wt. % viewed between crossed polarizers; the sample appeared colored and fragmented, and was very viscous. CTA-CNCs-50% did not phase separate to give the biphasic isotropic and anisotropic phases that occur spontaneously in aqueous CNC suspensions above a critical concentration, but rather a continuous chiral nematic gel-like phase was observed. Possibly the continuous ordered phase indicates that at 6 wt. % we are beyond the biphasic region for this system. It is unclear why we did not observe a biphasic suspension at lower concentrations.

A fingerprint texture characteristic to chiral nematic liquid crystals, including CNCs in aqueous suspension, was apparent when the CTAB-modified sample was observed by polarized optical microscopy (*Fig 8b*). The texture was polychromatic and complex, with some regions showing ordered microdomains, and others characterized by longer regions of order. The chiral nematic pitch of the 6 wt. % CTA-CNCs-50% suspension in ethanol was ~4 μm, similar to the ~3 μm observed for a 10 wt. % suspension of neat commercial CNCs (note: at 6 wt. % the unmodified commercial sample appeared completely isotropic). The persistence of shear birefringence in the sample (*Fig 8c*) is likely due to the greater viscosity.

## Rheology

The viscosity as a function of shear stress was measured using the cone and plate geometry for native CNCs in water and CTA-CNCs in ethanol in order to quantify the increase in viscosity that was apparent after modification. Overall, CTA-CNCs-100% was the most viscous of the samples studied.

Fig 9 compares the viscosity of neat CNCs and CTA-CNCs-50%, ranging in concentration from 1-4 wt. % (experimental repeats are plotted on top of each other to indicate the reproducibility of the measurements). The viscosity is greater for the modified CNCs compared to the neat CNCs, and at concentrations > 1wt. %, significant shear thinning is observed for CTA-CNCs-50%. Visually, suspensions of CTA-CNCs-50% in ethanol at 1 and 4 wt. % were similar in appearance (photographs shown in Fig 9 inset) despite the difference in the dynamic viscosity profile.

Fig 10 compares the dynamic viscosity of the three different CTAB modified samples at 1 wt.%. The increased viscosity and shear thinning behavior measured for CTA-CNCs-70% and CTA-CNCs-100% is mirrored in the figure inset which shows the samples inverted at 1 wt.%; CTA-CNCs-70% and CTA-CNCs-100% gel upon standing (ca. 30 min), but easily revert back to a freely flowing fluid when shaken. The early onset of gelation (ca. 1 wt. %) for the ethanolic suspensions of CTA-CNCs-70% and CTA-CNCs-100% is in contrast to the gelation of neat CNCs which typically occurs at concentrations approaching 10 wt. %. The early onset of gelation may be related to the interaction between surfactant tails of neighboring CNCs as the suspension is concentrated, and/or to the increase in volume fraction of rods caused by the extended conformation of the surfactant in ethanol.

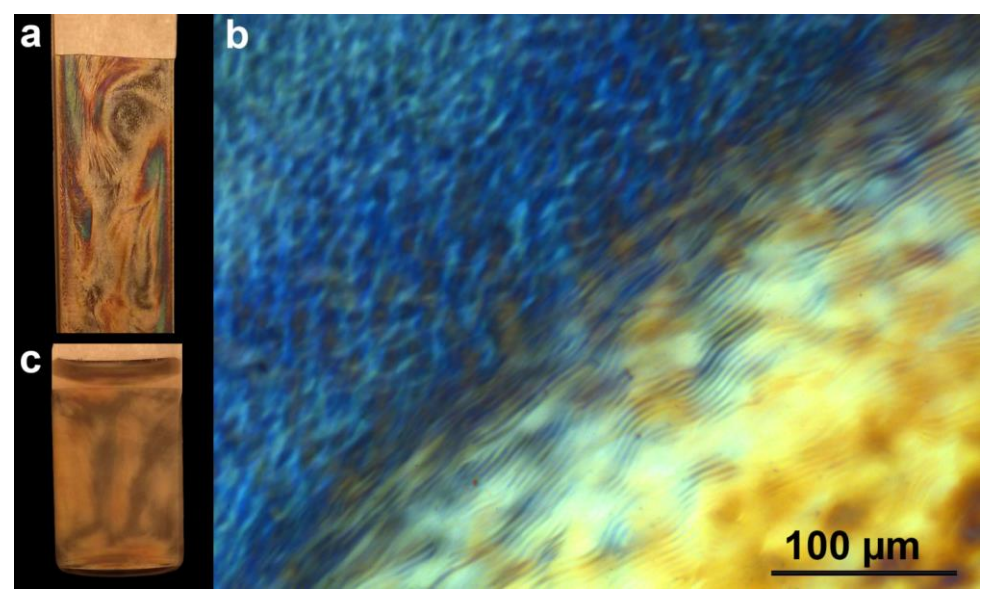


Fig 8 - CTA-CNCs-50% at 6 wt.% in a sealed microslide viewed between crossed polarizers (a) and in the polarized microscope (b), and CTA-CNCs-50% at 2 wt. % in a glass vial that was shaken prior to taking the photograph (c).

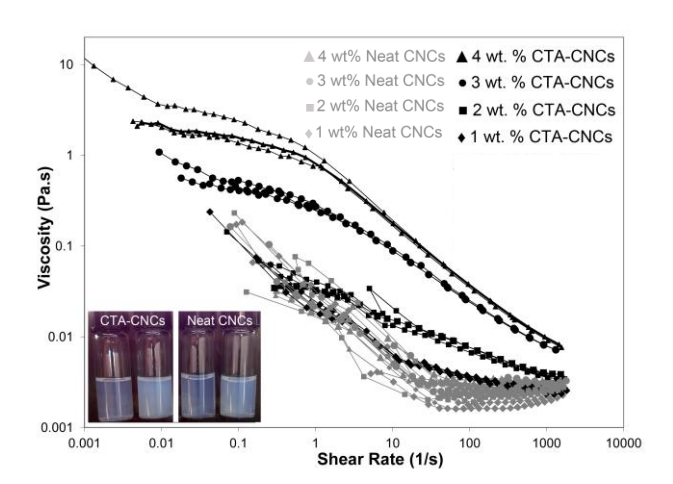


Fig 9 - Viscosity as a function of shear rate for neat CNCs in water (commercial source) and CTA-CNCs-50% in ethanol at concentrations ranging from 1-4 wt. %. Inset shows photographs of CTA-CNCs and neat CNCs at 1 and 4 wt. %.

# **Conclusions**

CNCs were surface-modified through adsorption with CTAB followed by purification to remove nonelectrostatically bound surfactant. By varying the adsorption reaction conditions, 50-100% charge coupling efficiency was achieved. The CTAB-modified CNCs formed stable suspensions in ethanol, exhibited chiral nematic phases, and, compared with native CNCs had a higher water contact angle and were more viscous. This work suggests that given enough surfactant and time for adsorption, 100% charge coupling can be obtained, however, ionic strength can hinder adsorption. It is expected that these findings are likely applicable to other cationic surfactants, and that by increasing the hydrophobic portion of the surfactant and/or the surface charge density on cellulose, CNCs can be dispersed in solvents or matrices of decreasing polarity.

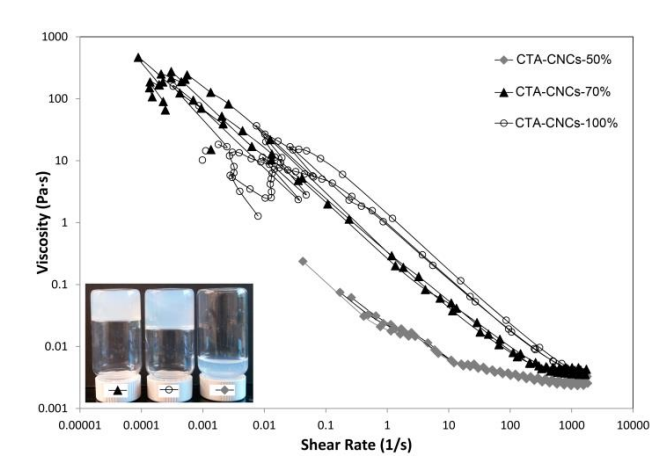


Fig 10 - Comparison of the viscosity as a function of shear rate for CTAB-modified CNC samples in ethanol at 1 wt. % concentrations. Inset photograph of ethanolic suspensions at 1 wt. % shows the gelation observed in samples reacted at 4:1 CTAB to sulfur (CTA-CNCs-70% and CTA-CNCs-100%).

#### Acknowledgements

The authors gratefully acknowledge Professors Guarne, Pelton, and Moran-Mirabal for access to instrumentation. R. Mafi is thanked for assistance with contact angle and rheology measurements.

#### Literature

(2013-2014): CRC Handbook of Chemistry and Physics, Taylor and Francis Group, LLC.

**Abitbol, T., Kloser, E. and Gray, D. G.** (2013): Estimation of the surface sulfur content of cellulose nanocrystals prepared by sulfuric acid hydrolysis, Cellulose, 20(2), 785-794.

**Alila, S., Aloulou, F., Beneventi, D. and Boufi, S.** (2007): Self-Aggregation of Cationic Surfactants onto Oxidized Cellulose Fibers and Coadsorption of Organic Compounds, Langmuir, 23(7), 3723-3731.

- Alila, S., Boufi, S., Belgacem, M. N. and Beneventi, D. (2005): Adsorption of a Cationic Surfactant onto Cellulosic Fibers I. Surface Charge Effects, Langmuir, 21(18), 8106-8113.
- **Araki, J., Wada, M. and Kuga, S.** (2000a): Steric Stabilization of a Cellulose Microcrystal Suspension by Poly(ethylene glycol) Grafting, Langmuir, 17(1), 21-27.
- **Araki, J., Wada, M., Kuga, S. and Okano, T.** (2000b): Birefringent Glassy Phase of a Cellulose Microcrystal Suspension, Langmuir, 16(2413-2415.
- **Beck-Candanedo, S., Roman, M. and Gray, D. G.** (2005): Effect of reaction conditions on the properties and behavior of wood cellulose nanocrystal suspensions, Biomacromolecules, 6(2), 1048-1054.
- **Boluk, Y., Zhao, L. and Incani, V.** (2012): Dispersions of Nanocrystalline Cellulose in Aqueous Polymer Solutions: Structure Formation of Colloidal Rods, Langmuir, 28(14), 6114-6123.
- **Bondeson, D. and Oksman, K.** (2007a): Dispersion and characteristics of surfactant modified cellulose whiskers nanocomposites, Composite Interfaces, 14(7-9), 617-630.
- **Bondeson, D. and Oksman, K.** (2007b): Polylactic acid/cellulose whisker nanocomposites modified by polyvinyl alcohol, Composites Part A: Applied Science and Manufacturing, 38(12), 2486-2492.
- Bonini, C., Heux, L., Cavaillé, J.-Y., Lindner, P., Dewhurst, C. and Terech, P. (2002): Rodlike Cellulose Whiskers Coated with Surfactant: A Small-Angle Neutron Scattering Characterization, Langmuir, 18(8), 3311-3314.
- **Brito, B. L., Pereira, F., Putaux, J.-L. and Jean, B.** (2012): Preparation, morphology and structure of cellulose nanocrystals from bamboo fibers, Cellulose, 19(5), 1527-1536.
- Cranston, E. D., Gray, D. G. and Rutland, M. W. (2010): Direct Surface Force Measurements of Polyelectrolyte Multilayer Films Containing Nanocrystalline Cellulose, Langmuir, 26(22), 17190-17197.
- **Derjaguin, B. and Landau, L.** (1993): Theory of the stability of strongly charged lyophobic sols and of the adhesion of strongly charged particles in solutions of electrolytes, Progress in Surface Science, 43(1–4), 30-59.
- **Dhar, N., Au, D., Berry, R. C. and Tam, K. C.** (2012): Interactions of nanocrystalline cellulose with an oppositely charged surfactant in aqueous medium, Colloids and Surfaces A: Physicochemical and Engineering Aspects, 415(0), 310-319.
- **Dong, X. M., Revol, J. F. and Gray, D. G.** (1998): Effect of microcrystallite preparation conditions on the formation of colloid crystals of cellulose, Cellulose, 5(1), 19-32.
- **Dufresne, A.** (2010): Processing of Polymer Nanocomposites Reinforced with Polysaccharide Nanocrystals, Molecules, 15(4111-4128.
- **Dugan, J. M., Gough, J. E. and Eichhorn, S. J.** (2010): Directing the Morphology and Differentiation of Skeletal Muscle Cells using Oriented Cellulose Nanowhiskers, Biomacromolecules, 11(2498-2504.
- **Elazzouzi-Hafraoui, S., Putaux, J.-L. and Heux, L.** (2009): Self-assembling and Chiral Nematic Properties of Organophilic Cellulose Nanocrystals, The Journal of Physical Chemistry B, 113(32), 11069-11075.

- Goussé, C., Chanzy, H., Cerrada, M. L. and Fleury, E. (2004): Surface silylation of cellulose microfibrils: preparation and rheological properties, Polymer, 45(5), 1569-1575.
- Goussé, C., Chanzy, H., Excoffier, G., Soubeyrand, L. and Fleury, E. (2002): Stable suspensions of partially silylated cellulose whiskers dispersed in organic solvents, Polymer, 43(9), 2645-2651.
- **Grunert, M. and Winter, W.** (2002): Nanocomposites of Cellulose Acetate Butyrate Reinforced with Cellulose Nanocrystals, Journal of Polymers and the Environment, 10(1-2), 27-30.
- **Habibi, Y., Lucia, L. A. and Rojas, O. J.** (2010): Cellulose Nanocrystals: Chemistry, Self-Assembly, and Applications, Chemical Reviews, 110(6), 3479-3500.
- **Heux, L., Chauve, G. and Bonini, C.** (2000): Nonflocculating and Chiral-Nematic Self-Ordering of Cellulose Microcrystals Suspensions in Nonpolar Solvents, Langmuir, 16(8210-8212.
- Hubbe, M. A., Rojas, O. J., Lucia, L. A. and Sain, M. (2008): Cellulosic nanocomposites: a review, BioResources, 3(3), 929-980.
- Jackson, J. K., Letchford, K., Wasserman, B. Z., Ye, L., Hamad, W. Y. and Burt, H. M. (2011): The use of nanocrystalline cellulose for the binding and controlled release of drugs, International journal of nanomedicine, 6(321.
- Junior de Menezes, A., Siqueira, G., Curvelo, A. A. S. and Dufresne, A. (2009): Extrusion and characterization of functionalized cellulose whiskers reinforced polyethylene nanocomposites, Polymer, 50(19), 4552-4563.
- Kalashnikova, I., Bizot, H., Cathala, B. and Capron, I. (2011): Modulation of Cellulose Nanocrystals Amphiphilic Properties to Stabilize Oil/Water Interface, Biomacromolecules, 13(1), 267-275.
- Kan, K. H. M., Li, J., Wijesekera, K. and Cranston, E. D. (2013): Polymer-Grafted Cellulose Nanocrystals as pH Responsive Reversible Flocculants. , Biomacromolecules, DOI: 10.1021/bm400752k(
- Kelly, J. A., Shukaliak, A. M., Cheung, C. C. Y., Shopsowitz, K. E., Hamad, W. Y. and MacLachlan, M. J. (2013): Responsive Photonic Hydrogels Based on Nanocrystalline Cellulose, Angewandte Chemie International Edition, 52(34), 8912-8916.
- Kim, J., Montero, G., Habibi, Y., Hinestroza, J. P., Genzer, J., Argyropoulos, D. S. and Rojas, O. J. (2009): Dispersion of cellulose crystallites by nonionic surfactants in a hydrophobic polymer matrix, Polymer Engineering & Science, 49(10), 2054-2061.
- Klemm, D., Kramer, F., Moritz, S., Lindstrom, T., Ankerfors, M., Gray, D. and Dorris, A. (2011): Nanocelluloses: A New Family of Nature-Based Materials, Angewandte Chemie-International Edition, 50(24), 5438-5466.
- **Kloser, E. and Gray, D. G.** (2010): Surface Grafting of Cellulose Nanocrystals with Poly(ethylene oxide) in Aqueous Media, Langmuir, 26(16), 13450-13456.
- Lam, E., Male, K. B., Chong, J. H., Leung, A. C. W. and Luong, J. H. T. (2012): Applications of functionalized and nanoparticle-modified nanocrystalline cellulose, Trends in Biotechnology, 30(5), 283-290.

- Leung, A. C. W., Hrapovic, S., Lam, E., Liu, Y., Male, K. B., Mahmoud, K. A. and Luong, J. H. T. (2011): Characteristics and Properties of Carboxylated Cellulose Nanocrystals Prepared from a Novel One-Step Procedure, Small, 7(3), 302-305
- Liang, H., Miranto, H., Granqvist, N., Sadowski, J. W., Viitala, T., Wang, B. and Yliperttula, M. (2010): Surface plasmon resonance instrument as a refractometer for liquids and ultrathin films, Sensors and Actuators B: Chemical, 149(1), 212-220.
- **Lindman, B., Karlström, G. and Stigsson, L.** (2010): On the mechanism of dissolution of cellulose, Journal of Molecular Liquids, 156(1), 76-81.
- Liu, J.-F., Min, G. and Ducker, W. A. (2001): AFM Study of Cationic Surfactants and Cationic Polyelectrolytes at the Silica-Water Interface, Langmuir, 17(4895-4903.
- Ljungberg, N., Bonini, C., Bortolussi, F., Boisson, C., Heux, L. and Cavaillé (2005): New Nanocomposite Materials Reinforced with Cellulose Whiskers in Atactic Polypropylene: Effect of Surface and Dispersion Characteristics, Biomacromolecules, 6(5), 2732-2739.
- **Ljungberg, N., Cavaillé, J. Y. and Heux, L.** (2006): Nanocomposites of isotactic polypropylene reinforced with rod-like cellulose whiskers, Polymer, 47(18), 6285-6292.
- McDermott, D. C., Kanelleas, D., Thomas, R. K., Rennie, A. R., Satija, S. K. and Majkrzak, C. F. (1993): Study of the adsorption from aqueous solution of mixtures of nonionic and cationic surfactants on crystalline quartz using the technique of neutron reflection, Langmuir, 9(9), 2404-2407.
- Moon, R. J., Martini, A., Nairn, J., Simonsen, J. and Youngblood, J. (2011): Cellulose nanomaterials review: structure, properties and nanocomposites, Chemical Society Reviews, 40(7), 3941-3994.
- **Notley, S. M. and Norgren, M.** (2006): Measurement of Interaction Forces between Lignin and Cellulose as a Function of Aqueous Electrolyte Solution Conditions, Langmuir, 22(26), 11199-11204.
- Padalkar, S., Capadona, J. R., Rowan, S. J., Weder, C., Won, Y.-H., Stanciu, L. A. and Moon, R. J. (2010): Natural Biopolymers: Novel Templates for the Synthesis of Nanostructures, Langmuir, 26(11), 8497-8502.
- Penfold, J., Tucker, I., Petkov, J. and Thomas, R. K. (2007): Surfactant Adsorption onto Cellulose Surfaces, Langmuir, 23(16), 8357-8364.
- **Peng, B. L., Dhar, N., Liu, H. L. and Tam, K. C.** (2011): Chemistry and applications of nanocrystalline cellulose and its derivatives: A nanotechnology perspective, The Canadian Journal of Chemical Engineering, 89(5), 1191-1206.
- **Petersson, L., Kvien, I. and Oksman, K.** (2007): Structure and thermal properties of poly(lactic acid)/cellulose whiskers nanocomposite materials, Composites Science and Technology, 67(11–12), 2535-2544.

- Revol, J. F., Bradford, H., Giasson, J., Marchessault, R. H. and Gray, D. G. (1992): Helicoidal Self-Ordering of Cellulose Microfibrils in Aqueous Suspension, International Journal of Biological Macromolecules, 14(3), 170-172.
- Revol, J. F., Godbout, L., Dong, X. M. and Gray, D. G. (1994a): Chiral nematic suspensions of cellulose crystallites; phase separation and magnetic field orientation, Liquid Crystals, 16(1), 127-134.
- Revol, J. F., Godbout, L., Dong, X. M., Gray, D. G., Chanzy, H. and Maret, G. (1994b): Chiral Nematic Suspensions of Cellulose Crystallites Phase-Separation and Magnetic-Field Orientation, Liquid Crystals, 16(1), 127-134.
- Rusli, R., Shanmuganathan, K., Rowan, S. J., Weder, C. and Eichhorn, S. J. (2011): Stress Transfer in Cellulose Nanowhisker Composites-Influence of Whisker Aspect Ratio and Surface Charge, Biomacromolecules, 12(4), 1363-1369.
- **Salajková, M., Berglund, L. A. and Zhou, Q.** (2012): Hydrophobic cellulose nanocrystals modified with quaternary ammonium salts, Journal of Materials Chemistry, 22(37), 19798-19805.
- **Shopsowitz, K. E., Qi, H., Hamad, W. Y. and MacLachlan, M. J.** (2010): Free-standing mesoporous silica films with tunable chiral nematic structures, Nature, 468(422-426.
- **Siqueira, G., Bras, J. and Dufresne, A.** (2010a): Cellulosic Bionanocomposites: A Review of Preparation, Properties and Applications, Polymers, 2(728-765.
- Siqueira, G., Tapin-Lingua, S., Bras, J., da Silva Perez, D. and Dufresne, A. (2010b): Morphological investigation of nanoparticles obtained from combined mechanical shearing, and enzymatic and acid hydrolysis of sisal fibers, Cellulose, 17(6), 1147-1158.
- Syverud, K., Xhanari, K., Chinga-Carrasco, G., Yu, Y. and Stenius, P. (2011): Films made of cellulose nanofibrils: surface modification by adsorption of a cationic surfactant and characterization by computer-assisted electron microscopy, Journal of Nanoparticle Research, 13(2), 773-782.
- **Verwey, E. J. W. and Overbeek, J. T. G.** (1948): Theory of the stability of lyophobic colloids, Elsevier, Amsterdam.
- Wang, H., Qian, C. and Roman, M. (2011): Effects of pH and Salt Concentration on the Formation and Properties of Chitosan–Cellulose Nanocrystal Polyelectrolyte–Macroion Complexes, Biomacromolecules, 12(10), 3708-3714.
- **Xhanari, K., Syverud, K., Chinga-Carrasco, G., Paso, K. and Stenius, P.** (2011): Reduction of water wettability of nanofibrillated cellulose by adsorption of cationic surfactants, Cellulose, 18(2), 257-270.
- Yuan, H., Nishiyama, Y., Wada, M. and Kuga, S. (2006): Surface Acylation of Cellulose Whiskers by Drying Aqueous Emulsion, Biomacromolecules, 7(3), 696-700.
  - Manuscript received November 27, 2013 Accepted January 13, 2014